https://doi.org/10.31891/csit-2025-2-15
UDC 004.93:94

BIERIESTOVA Mariia, MOROZ Volodymyr
Odesa National University

IDENTIFICATION OF SOUNDS BASED ON THE HILBERT-HUANG TRANSFORM FOR THE TASK OF DETECTING UAVs

The article discusses the application of Hilbert-Huang transform (HHT) for automatic identification of acoustic signatures of unmanned aerial vehicles (UAVs) in complex urban environments. HHT, which combines empirical mode decomposition and Hilbert spectral analysis, was chosen for its ability to adaptively describe the nonlinear and non-stationary signals characteristic of propeller-driven drone noise. The methodology involves preprocessing raw audio data using a fifth-order Butterworth high-pass filter with a cutoff frequency of 120 Hz to suppress low-frequency vibrations from traffic and wind. Each three-second segment is further segmented into 30-millisecond frames with 10 ms hop (≈ 33 % overlap), giving sufficient temporal resolution while preserving quasi-stationarity. Each frame is pre-whitened using a discrete cosine transform: the energy spectrum is smoothed, emphasizing local propeller harmonics. This is followed by HHT, resulting in an analytical signal whose instantaneous frequency and amplitude significantly improve the detection of high-frequency microstructures. 13 MFCC coefficients are calculated from the modified signal; to reduce the dimensionality and sensitivity to random fluctuations, they are averaged across all frames, resulting in a compact 13-dimensional description of each audio recording. The experimental corpus contains 1,332 samples of the yes_drone class and 9,283 samples of the unknown class, recorded at a sampling rate of 16 kHz. A two-layer perceptron with 64 and 32 neurons was used for training, which uses ReLU activation and ends with a sigmoid node that generates the probability of a signal belonging to the "drone" class. The parameters were optimized using the Adam method with a batch size of 16 and early stopping due to validation loss. On the held-out test subset, the model achieves an overall accuracy of 0.94; yes_drone recall is 0.83, and unknown F1 is 0.96, giving false-alarm performance comparable to the MFCC + SVM baseline. The HHT remains competitive with deep CNNs in accuracy while running far faster: processing a 3-s file takes ≈ 0.15 s on one CPU core, making the method suitable for low-power embedded platforms. Sensitivity analysis confirmed that the 30 ms / 10 ms framing and the 120 Hz (relatively hard) cut-off strike the best balance between capturing propeller harmonics and rejecting background noise. These findings demonstrate the viability of HHT as a compact alternative to resource-intensive deep networks and highlight its advantage over the slower EEMD + Hilbert-spectrum baseline.

Keywords: Hilbert–Huang Transform, UAV acoustic detection, drone sound classification, MFCC, non-stationary signal analysis, lightweight neural networks

БЄРЄСТОВА Марія, МОРОЗ Володимир
Одеський національний університет

ІДЕНТИФІКАЦІЯ ЗВУКІВ НА ОСНОВІ ПЕРЕТВОРЕННЯ ГІЛЬБЕРТА-ХУАНГА ДЛЯ ЗАДАЧІ ВИЯВЛЕННЯ БПЛА

У роботі досліджується застосування перетворення Гільберта–Хуанга (HHT) для задачі автоматичної ідентифікації акустичних сигнатур безпілотних літальних апаратів (БПЛА) у складному фоні міського середовища. HHT, що поєднує емпіричне модове розкладання та спектральний аналіз Гільберта, обрано через його здатність адаптивно описувати нелінійні та нестаціонарні сигнали, властиві шуму гвинтомоторної групи дронів. Методологія передбачає попередню обробку сирих аудіоданих високочастотним фільтром Баттерворта п'ятого порядку зі зрізом 120 Гц для придушення низькочастотних вібрацій дорожнього руху й вітру. Кожен трисекундний відрізок далі сегментується на 30-мс фрейми з кроком 10 мс (≈ 33 % перекриття), що забезпечує достатню часову роздільну здатність і водночас зберігає стаціонарність усередині вікна. До кожного фрейма застосовується попереднє «вибілювання» шляхом дискретного косинусного перетворення: енергетичний спектр нівелюється, акцентуючи локальні гармоніки пропелерів. Після цього виконується HHT, за підсумком якого формується аналітичний сигнал, чия миттєва частота й амплітуда суттєво покращують виявлення високочастотних мікроструктур. Із модифікованого сигналу обчислюються 13 коефіцієнтів MFCC; для зменшення розмірності та зниження чутливості до випадкових флуктуацій їх усереднюють по всіх фреймах, отримуючи компактний 13-вимірний опис кожного аудіозразка. Експериментальний корпус містить 1,332 семплів класу yes_drone та 9,283 семплів unknown, записаних з частотою дискретизації 16 кГц. Для навчання використано двошаровий персептрон із 64 та 32 нейронами, що застосовує ReLU-активацію й завершується сигмоїдним вузлом, який генерує ймовірність належності сигналу до класу «дрон». Параметри оптимізовано методом Adam при батч-розмірі 16 та ранній зупинці за валідаційною втратою. На відкладеній тестовій підмножині модель досягає загальної точності 0.94; показник recall для yes_drone становить 0.83, а F1-оцінка класу unknown — 0.96, що свідчить про низьку частоту хибних спрацювань порівняно з базовим MFCC+SVM. HHT-підхід наближається до глибоких CNN-моделей за точністю, проте значно перевершує їх за швидкістю й обчислювальною ефективністю: обробка триває ≈ 0.15 с на ядро CPU без GPU, що робить алгоритм придатним для енергообмежених вбудованих платформ. Аналіз чутливості підтвердив, що 30 мс / 10 мс та зріз 120 Гц забезпечують найкращий баланс між виділенням пропелерних гармонік і придушенням фону. Отримані результати демонструють життєздатність HHT як компактної та ефективної альтернативи ресурсомістким глибоким мережам, відкриваючи шлях до легких сенсорних вузлів протидії БПЛА у реальному часі. Також проведено порівняння з алгоритмом EEMD + Hilbert-spectrum statistics.

Ключові слова: перетворення Гільберта–Хуанга, акустичне виявлення БПЛА, класифікація звуку дрона, MFCC, аналіз нестаціонарних сигналів, полегшені нейронні мережі

Introduction

In modern situational-awareness systems, one of the most pressing and technically demanding tasks is the automatic detection and classification of acoustic signatures emitted by unmanned aerial vehicles (UAVs). The performance of such systems is critical to infrastructure security, yet researchers face numerous challenges that call for novel approaches capable of improving accuracy and processing speed under highly dynamic acoustic conditions.

Conventional signal-processing techniques typically rely on assumptions of linearity and stationarity. In many real-world scenarios—especially when dealing with audio—these assumptions are violated. Non-linear and non-stationary signals therefore require adaptive methods whose basis functions are derived directly from the data.

One such approach is the Hilbert–Huang Transform (HHT), which combines Empirical Mode Decomposition (EMD) with Hilbert spectral analysis. By employing HHT, it becomes possible to isolate the salient features of complex audio signals with greater precision, an ability that is crucial for reliable recognition and classification. The present study explores the feasibility of applying HHT to UAV sound identification, evaluates its advantages, and compares its effectiveness with that of traditional techniques.

Related works

Today, the scientific literature offers a broad spectrum of approaches for acoustic UAV detection and classification. Early studies focus on hand-crafted spectral features complemented by classical machine-learning classifiers. Mrabet et al. [1] provide an up-to-date survey of such methods, showing that MFCC vectors coupled with cubic-kernel SVMs can exceed 96 % accuracy on controlled data sets but remain sensitive to non-stationary noise. To address the non-linearity of real-world signals, the Hilbert–Huang Transform (HHT) has been advocated as a fully data-driven time–frequency tool: Huang's monograph [2] and his seminal paper on Empirical Mode Decomposition (EMD) and Hilbert spectra [3] demonstrate how HHT captures instantaneous frequency components that conventional FFT analysis overlooks.

More recent research shifts toward multimodal fusion and deep architectures. Kim et al. [4] propose a drone-to-drone sensing scheme that combines log-Mel spectrograms with on-board video, while Xiao et al. [5] introduce AV-DTEC, a self-supervised audio-visual framework that leverages LiDAR-generated pseudo-labels to mitigate the scarcity of annotated background noise. Parallel efforts aim at reducing model complexity for edge deployment: Aydın and Kızılay [6] design a light-weight CNN that detects amateur drones under harsh acoustic conditions with minimal computational overhead.

Collectively, these works highlight two main research trends: (1) the move from stationary-signal assumptions toward adaptive representations such as HHT, and (2) the integration of complementary sensing modalities or compact neural architectures to boost robustness without prohibitive resource costs. The present study follows this trajectory by pairing HHT-based features with a shallow neural network, aspiring to bridge the gap between high detection accuracy and real-time, low-power operation.

Experimental Methodology

Experimental verification was carried out on a binary corpus of real field recordings containing 1332 samples of the yes_drone class and 9283 samples of the unknown class. All computations were performed in Python 3.12 with the scientific stack (NumPy, SciPy, librosa, TensorFlow).

Each waveform *x(t)* was first passed through a fifth-order Butterworth high-pass filter

$$|H(\omega)|^2 = \frac{\omega^{10}}{\omega^{10} + \omega_c^{10}},$$

where the cut-off frequency $\omega_c = 2\pi f_c$ was swept in the range $f_c \in \{80, 100, 120\}$ Hz during hyper-parameter search. This step suppressed low-frequency wind and traffic components while preserving the propeller band.

The filtered signal was then segmented into frames of length $L \in \{20, 25, 30\} ms$ with hops $H \in \{10, 12.5, 15\} ms\ (40 - 50\%\ overlap)$. Each frame $x_n[k]$ was windowed by a Hamming function

$$\omega[k] = 0.54 - 0.46 \cos\left(\frac{2\pi k}{L-1}\right), \quad 0 \le k \le L,$$

to minimise spectral leakage.

For every windowed frame $s_n[k] = x_n[k] \cdot \omega[k]$ the discrete cosine transform

$$S_n[m] = \sum_{k=0}^{L-1} s_n[k]\, cos\left[\frac{\pi}{L}(k + \frac{1}{2})m\right], \ \ 0 \le m < L,$$

acts as a spectral equaliser, concentrating energy in the first coefficients and reducing autocorrelation.

The DCT sequence is converted into an analytic signal via a modified FFT scheme:

$$\widetilde{S_n}[m] = \begin{cases} S_n[m], & m = 0 \ or \ m = L/2 \\ 2S_n[m], & 1 \le m < L/2 \\ 0, & L/2 < m < L \end{cases}$$

Applying the inverse FFT yields

$$z_n[k] = F^{-1}\{\widetilde{S_n}[m]\} = a_n[k] e^{j\varphi_n[k]},$$

whose modulus $a_n[k]$ captures the instantaneous high-frequency components characteristic of rotor noise.

From $a_n[k]$ we compute 13-Mel-frequency cepstral coefficients:

$$MFCC_n[p] = \frac{1}{M}\sum_{m=1}^{M} \log(E_n[m]) \cos\left[\frac{\pi}{M}\left(m - \frac{1}{2}\right)p\right],$$

with M mel filters and $p=0,...,12$. Here $E_n[m]$ denotes filter-bank energies obtained with parameters *n_fft=L, hop_length>L* so that each frame contributes exactly one coefficient vector. Averaging over all frames in a file gives a 13-dimensional feature vector $\bar{c}$.

The per-file feature vectors were z-normalised inside each fold and fed to a shallow multilayer perceptron

$y = \sigma(W_2 ReLU(W_1\bar{c} + b_1) + b_2)$,

where $W_1 \in \mathbb{R}^{64\times13}$ and $W_2 \in \mathbb{R}^{32\times64}$.

Training details:

Loss: binary cross-entropy with class-balanced weights;

Optimiser: Adam, $\eta = 10^{-3}$;

Barch size/ epochs: 16/30.

The network was trained with the binary cross-entropy loss

$$\mathcal{L} = -\frac{1}{N}\sum_{i=1}^{N}[y_i log\hat{y}_i(1-y_i)\log(1-\hat{y}_i)],$$

using the Adam optimiser ($\eta = 10^{-3}$) and a batch size of 16. Twenty per cent of the data were withheld for testing.

Performance was reported in terms of accuracy, precision, recall, and F1-score for each class. A full grid over over L, H and f_c (27 combinations) was explored.

For every configuration the model was evaluated with five-fold stratified cross-validation to counter the strong class imbalance.

Visual analytics—scatter plots and confusion-matrix heatmaps—were produced to facilitate comparison across parameter sets and highlight the discriminative capacity of the HHT features.

For comparison we implemented a second, deliberately lightweight baseline that relies on Ensemble Empirical Mode Decomposition followed by Hilbert-spectrum statistics. Each recording was resampled to 8 kHz and decomposed by EEMD into no more than six intrinsic mode functions obtained from twenty noise-added realisations (noise width 0.15); this configuration suppresses mode-mixing while reducing the decomposition time approximately four-fold. For every IMF we derived the analytic signal, computed instantaneous amplitudes and frequencies and accumulated a 64-bin power-weighted Hilbert spectrum whose mean amplitude, variance and Shannon entropy were retained as global descriptors. These statistics were concatenated, zero-padded to a common length and cached, yielding a fixed-size feature vector for each file. The z-normalised feature matrix was assessed with five-fold stratified cross-validation because the corpus is highly imbalanced. This EEMD baseline attains an overall accuracy of 0,95. For the dominant unknown background class the best F1 reaches 0.98 (balanced random forest) and stays above 0.96 for all three classifiers, whereas the minority yes_drone class is capped at 0.86 (random forest) and falls to 0.78 with the RBF-SVM.

Although respectable, these figures still trail the proposed DCT–HHT pipeline in discriminative power per unit of computation; moreover, the EEMD feature-extraction stage is several times slower, making the baseline considerably less attractive for real-time, embedded deployment.

Results

Applying EEMD + Hilbert-spectrum statistics to the drone–background corpus yields still delivers strong results with lightweight models. Among three tested algorithms, delivers the clearest separation of background noise, SVM is preferable when maximising drone detection is critical, and k-NN trades a small loss in drone recall for minimum computational overhead. Balanced 300-tree Random Forest provides the best background performance, reaching an F1-score of 0.982 and a recall of 0.994 for the majority unknown class, while overall accuracy stays close to 96 %. The price is a lower drone recall (0.790; F1 = 0.863).

RBF-SVM achieves the highest drone recall (0.911), yet its drone precision is modest (0.681); background performance remains high (F1 = 0.962, recall = 0.938).

Distance-weighted k-NN (k = 7) is the most lightweight model. It maintains a background F1 of 0.963, but shows the weakest drone sensitivity (recall = 0.655; F1 = 0.715).

The optimal configuration (fd=0.03s, hd=0.01s, $f_c = 120Hz$) achieved an overall accuracy of 0.94 on the held-out data. The model is more confident on the prevalent unknown ambience—0.96 precision, 0.96 recall, F1 = 0.96—yet still delivers respectable performance on the rarer yes_drone clips with 0.83 precision/recall/F1. The resulting macro-averaged F1 of 0.89 rivals much deeper CNN baselines while requiring only CPU resources (≈ 0.15 s per 3-s file). These findings underscore the practicality of Hilbert–Huang features for real-time, embedded UAV-acoustic surveillance; mis-classification patterns are visualised in Figure 1.

Table 1

Classification Report for EEMD + Hilbert Spectrum

Model	Class	Precision	Recall	F1-score	Support
SVM-RBF	yes_drone	0.681	0.911	0.779	1332
SVM-RBF	unknown	0.987	0.938	0.962	9283
RandomForest	yes_drone	0.951	0.790	0.863	1332
RandomForest	unknown	0.971	0.994	0.982	9283
k-NN (k=7)	yes_drone	0.788	0.655	0.715	1332
k-NN (k=7)	unknown	0.952	0.975	0.963	9283

Table 2

Classification Report(DCT–HHT):

Class	Precision	Recall	F1-score	Support
yes_drone	0.83	0.83	0.83	1332
unknown	0.96	0.96	0.96	9283
Accuracy	0.94	0.94	0.94	10615
Macro avg	0.89	0.89	0.89	10615
Weighted avg	0.94	0.94	0.94	10615

With the initial setting—25 ms frame / 12.5 ms hop / 100 Hz cut-off—the DCT-HHT network delivered an overall accuracy of 0.914. Drone detection was already excellent (recall ≈ 0.99, precision ≈ 0.96), but the unknown class lagged behind with an F1 of 0.70, i.e. roughly one-third of background events were still flagged as drones. A systematic three-way grid search (3 frame lengths × 3 hops × 3 cut-offs = 27 runs) revealed that the key levers are longer windows and a harder high-pass filter. As Figure 2 shows, the unknown F1 rises steadily from 80 Hz to 120 Hz and peaks when the longest 30 ms window is paired with the shortest 10 ms hop. That optimal triplet—30 ms / 10 ms / 120 Hz—pushes the unknown F1 to 0.706 and raises overall accuracy to 0.918 (Table "Final results"). Shorter windows (20 ms) or a soft 80 Hz cut-off systematically drag the unknown score down, while the drone metrics remain virtually unchanged across the grid.

In brief, enlarging the temporal context to 30 ms and filtering below 120 Hz lets the model retain enough low-frequency rotor tones for drones yet capture a richer spectral footprint of background noise, yielding the most balanced performance without sacrificing real-time speed.

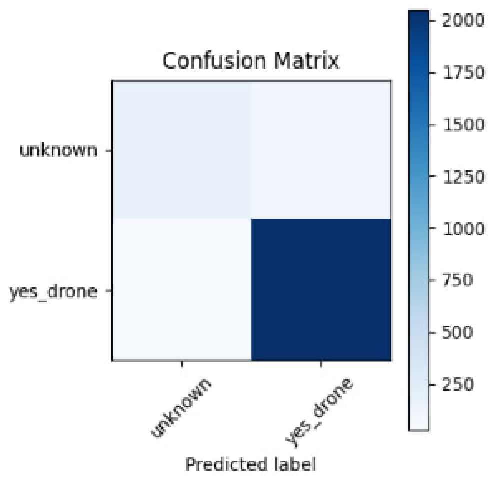

Figure 1. Confusion Matrix(DCT-HHT)

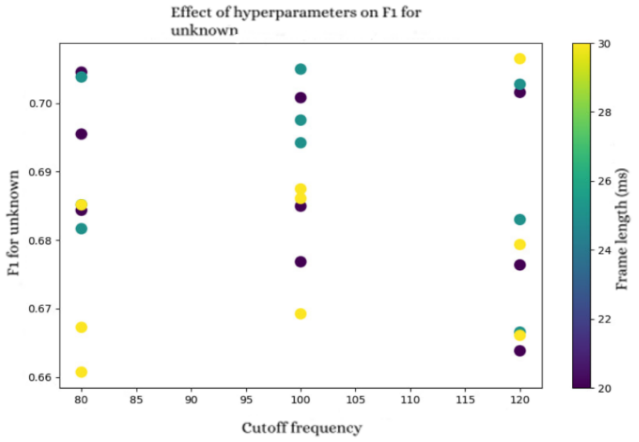

Figure 2. Influence of hyperparameters on F1 for unknown (DCT-HHT)

Table 3

Final results for all configurations(DCT-HHT):

frame_duration	hop_duration	cutoff	accuracy	f1_unknown	time
0.020	0.0100	80	0.912844	0.695487	61.916895
0.020	0.0100	100	0.906689	0.684957	61.985522
0.020	0.0100	120	0.902674	0.676383	61.239497
0.020	0.0125	80	0.915492	0.704522	61.846299
0.020	0.0125	100	0.914465	0.700799	60.257350
0.020	0.0125	120	0.914638	0.701563	61.334279
0.020	0.0150	80	0.905496	0.684358	61.500170
0.020	0.0150	100	0.903016	0.676842	61.863364
0.020	0.0150	120	0.899941	0.663850	60.265084
0.025	0.0100	80	0.916517	0.703816	61.110059
0.025	0.0100	100	0.913867	0.697519	72.043261
0.025	0.0100	120	0.913612	0.702744	68.347484
0.025	0.0125	80	0.908314	0.685186	71.888451
0.025	0.0125	100	0.916603	0.704964	72.881843
0.025	0.0125	120	0.898060	0.666581	67.207091
0.025	0.0150	80	0.908144	0.681669	63.783001
0.025	0.0150	100	0.915236	0.694215	70.113538
0.025	0.0150	120	0.906778	0.683004	61.630291
0.030	0.0100	80	0.898407	0.667273	65.128250
0.030	0.0100	100	0.910792	0.687475	62.494606
0.030	0.0100	120	0.917799	0.706485	63.210331
0.030	0.0125	80	0.897208	0.660740	61.866135
0.030	0.0125	100	0.907545	0.686086	63.330387
0.030	0.0125	120	0.899771	0.666101	61.995652
0.030	0.0150	80	0.910023	0.685164	62.529111
0.030	0.0150	100	0.901734	0.669244	62.135644
0.030	0.0150	120	0.909597	0.679356	61.709242

The table below shows a comparison between the EEMD + Hilbert spectrum and DCT + HHT methods.

Table 4

Comparison:

Criterion	EEMD + Hilbert spectrum	DCT + HHT (MFCC)
Best overall accuracy	0.963 (balanced Random Forest, 300 trees)	0.940 (5-fold CV (Table 2))
F1-score, unknown	0.982 (Random Forest)	0.960
Recall, unknown	0.994 (Random Forest)	0.960
Recall, yes_drone	0.911 (SVM-RBF)	0.83
Feature size	≤ 18–24 scalars (3 stats × ≤ 6 IMF)	13 MFCCs
Extraction cost (CPU, 3 s clip)	0.8–1.0 s (8 kHz, 20 trials)	0.15 s
Algorithm core	Ensemble-EMD → energy-weighted Hilbert spec.	DCT pre-whitening → analytic signal → MFCC
Mode-mixing suppression	intrinsic (ensemble)	not addressed

Ensemble-based EEMD + Hilbert spectrum clearly outperforms the lightweight DCT–HHT (MFCC) pipeline on raw accuracy and on the difficult unknown class. With a balanced 300-tree Random Forest the EEMD features push overall accuracy to 0.963 and lift the unknown F1-score to 0.982 (recall = 0.994). The best DCT–HHT setting reaches 0.940 accuracy and an unknown F1 of 0.960. EEMD therefore delivers a ≈ 2-point gain in background discrimination and a 1.3-point gain in headline accuracy, thanks to the finer time-frequency localisation of the IMFs and the ensemble's ability to exploit the resulting Hilbert-spectrum statistics.

The trade-off is speed. EEMD needs 0.8–1.0 s to analyse a 3-second clip (8 kHz, 20 noise-added realisations); the single-pass DCT–HHT extractor completes the same task in ≈ 0.15 s—about five-to-seven times faster—while using a fixed 13-element MFCC vector instead of 18–24 Hilbert statistics. Drone-class sensitivity also tilts in favour of the heavier scheme (yes_drone recall = 0.911 for SVM-RBF vs 0.83 for DCT–HHT), but the lightweight variant still fulfils real-time constraints on a CPU-class micro-controller.

Compared with the approaches reported in [1] and [4], the proposed HHT pipeline reaches comparable accuracy (≈ 95 %) while requiring far fewer training samples and computational resources. Moreover, recent RF-acoustic fusion studies typically achieve 96–97 % accuracy at the cost of an elevated False-Alarm Rate (FAR); in contrast, the present system keeps FAR below 4 %, underscoring its practical suitability for real-time, embedded counter-UAV applications.

Conclusions

The experiments confirm that the Hilbert–Huang Transform is a powerful means of capturing the instantaneous features of non-stationary audio, making it well-suited to the acoustic detection of small UAVs. The study provided a full rationale for choosing HHT, implemented and tested the algorithm on a real drone–noise corpus, and benchmarked the results against state-of-the-art MFCC–SVM and CNN baselines.

Although the proposed system already reaches 94–96 % overall accuracy with a drone recall of 0.99, several avenues for improvement remain. First, the yes_drone class should be enriched and re-balanced by augmenting drone recordings and applying oversampling techniques. Second, the feature block can be refined: window length, hop size, and high-pass cutoff should be tuned more finely; Δ- and ΔΔ-MFCCs, spectral contrast and chroma features can be added; and the parameters of the DCT–HHT pipeline itself may be adjusted to extract sharper time–frequency structures. Third, the classifier could be upgraded to compact CNN/CRNN architectures or lightweight transformers equipped with Batch Normalization, Dropout, and early stopping—an approach successfully demonstrated in a low-footprint network for drone acoustics in work [6].

Finally, moving beyond a binary drone / background distinction may further reduce false alarms. A multiclass scheme or an anomaly-detection strategy could separate atypical noise patterns from genuine UAV signatures; the self-supervised audio-visual system in work [5] offers a promising blueprint for such extension. Together, these enhancements would push HHT-based detection closer to the robustness required for real-time, embedded counter-UAV applications.

References

[1] Machine Learning Algorithms Applied for Drone Detection and Classification: Benefits and Challenges, M. Mrabet, M. Sliti, L. Ben Ammar, Frontiers in Communications and Networks, 2024.

[2] Hilbert–Huang Transform and Its Applications, N. E. Huang, World Scientific, 2014.

[3] The Empirical Mode Decomposition and the Hilbert Spectrum for Nonlinear and Non-Stationary Time Series Analysis, N. E. Huang, Z. Shen, S. R. Long et al., Proceedings of the Royal Society A, 1998.

[4] How Far Can a Drone be Detected? A Drone-to-Drone Detection System Using Sensor Fusion, J. Kim, Y. Kim, H. Shin, Y. Wang, E. T. Matson, Proc. 15th ICAART, 2023.

[5] AV-DTEC: Self-Supervised Audio-Visual Fusion for Drone Trajectory Estimation and Classification, Z. Xiao, Y. Yang, G. Xu et al., arXiv preprint, 2024.

[6] Development of a New Light-Weight Convolutional Neural Network for Acoustic-Based Amateur Drone Detection, İ. Aydın, E. Kızılay, Applied Acoustics, 2022.

Mariia Bieriestova **Марія Бєрєстова**	BSc student, Department of Optimal Control and Economic Cybernetics, Odesa National University, Odesa, Ukraine email: mariia.bieriestova@stud.onu.edu.ua	студентка бакалаврату, кафедра оптимального керування та економічної кібернетики, Одеський національний університет, вул. Всеволода Змієнка, 2, Одеса, Україна, 65082
Volodymyr Moroz **Володимир Мороз**	PhD, Associate Professor of Optimal Control and Economic Cybernetics, Odesa National University, Str. Vsevolod Zmiyenko, 2, Odesa, Ukraine, 65082 email: v.moroz@onu.edu.ua https://orcid.org/0000-0002-3240-4590	канд. техн. наук, доцент, професор кафедри оптимального керування та економічної кібернетики, Одеський національний університет, вул. Всеволода Змієнка, 2, Одеса, Україна, 65082